

Polarized light-by-light scattering at the CLIC induced by axion-like particles

S.C. İnan*

Department of Physics, Sivas Cumhuriyet University, 58140, Sivas, Turkey

and

A.V. Kisselev†

Division of Theoretical Physics, A.A. Logunov Institute for High Energy Physics,

NRC “Kurchatov Institute”, 142281, Protvino, Russia

Abstract

The light-by-light (LBL) scattering with initial polarized Compton backscattered photons at the CLIC, induced by axion-like particles (ALPs), is investigated. The total cross sections are calculated, assuming CP-even coupling of the pseudoscalar ALP to photons. The 95% C.L. exclusion region for the ALP mass m_a and its coupling constant f is presented. The results are compared with previously obtained CLIC bounds for the unpolarized case. It is shown that the bounds on f for the polarized beams in the region $m_a = 1000 \text{ GeV} - 2000 \text{ GeV}$, with the collision energy 3000 GeV and integrated luminosity 4000 fb^{-1} , are on average 1.5 times stronger than the bounds for the unpolarized beams. Herewith, our CLIC bounds are stronger than all current exclusion regions for $m_a > 80 \text{ GeV}$. In particular, they are more restrictive than the limits which follow from the ALP-mediated LBL scattering at the LHC.

*Electronic address: sceminan@cumhuriyet.tr

†Electronic address: alexandre.kisselev@ihep.ru

1 Introduction

The fine-tuning problem, known as the strong CP problem, is one of the open issues of the Standard Model (SM). It can be solved by introducing a spontaneously broken Peccei-Quinn symmetry [1, 2] which involves a light pseudoscalar particle, QCD axion [3, 4]. The QCD axion couples to the gluon field strength. Its phenomenology is determined by its low mass and very weak interactions. In particular, it could i) affect cosmology; ii) affect stellar evolution; iii) mediate new long-range forces; iv) be produced in a terrestrial laboratory. At present, the QCD axion is regarded as a main component of the dark matter [5]-[7]. The solar axion [8] has been proposed to explain the excess in the low-energy electron recoil observed by the XENON1T Collaboration [9], since its energy spectrum matches the excess.

An axion-like particle (ALP) is a particle having interactions similar to the axion. The origin of the ALP is expected to be similar but without the relationship between its coupling constant and mass. It means that the ALP mass can be treated independently of its couplings to the SM fields. The ALPs emerge in string theory scenarios [10]-[16], in theories with spontaneously broken symmetries [17, 18], or in the GUT [19]. All these models predict an ALP-photon coupling and, therefore, the electromagnetic decay of the ALPs in two photons. Experimental searches are mainly directed to ALPs, in order to relax the coupling parameter [20].

The heavy ALPs can be detected at colliders in a light-by-light (LBL) scattering [21]-[24]. It was shown that LHC searches with the use of the proton tagging technique constrain the ALP masses in the region 0.5 TeV – 2 TeV [23]-[25]. The current exclusion regions for the axion and ALP searches are shown in Fig. 1. The first evidence of the subprocess $\gamma\gamma \rightarrow \gamma\gamma$ was observed by the ATLAS [26, 27] and CMS [28] Collaborations in high-energy ultra-peripheral PbPb collisions. The phenomenological analysis of the exclusive and diffractive $\gamma\gamma$ production in PbPb scattering at the LHC and FCC was done in [29, 30]. The photon-induced process $pp \rightarrow p\gamma\gamma p \rightarrow p'\gamma\gamma p'$ at the LHC was studied in [31]-[33].

We have recently investigated the virtual production of the ALPs in the LBL scattering at the compact linear collider (CLIC) [34, 35] with the initial unpolarized Compton backscattered (CB) photons [36]. The 95% C.L. exclusion regions for the ALP mass m_a and ALP-photon coupling f have been calculated. It turned out that our CLIC bounds on m_a and f are stronger than the bounds for the LBL production of the ALP at the LHC presented

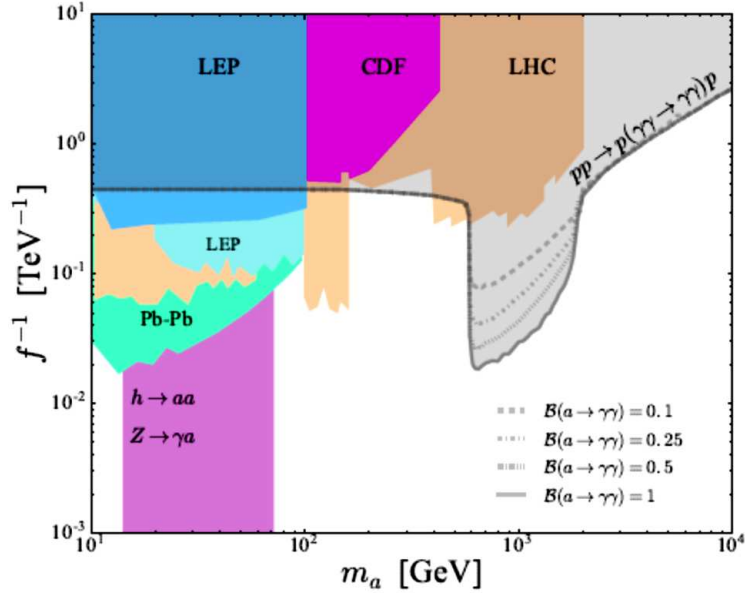


Figure 1: The 95% C.L. current exclusion regions for different values of the ALP branching $\text{Br}(a \rightarrow \gamma\gamma)$. Here f^{-1} is the ALP-photon coupling, and m_a is the ALP mass. The figure is taken from Ref. [23].

in Fig. 1. Thus, the ALP search at the CLIC has a great physics potential of searching for the ALPs, especially in the mass region 1 TeV – 2.4 TeV [36].

The CLIC is planned to accelerate and collide electrons and positrons at maximally 3 TeV center-of-mass energy. Three energy states of the CLIC with $\sqrt{s} = 380$ GeV, $\sqrt{s} = 1500$ GeV and $\sqrt{s} = 3000$ GeV are considered. The expected integrated luminosities are $L = 1000 \text{ fb}^{-1}$, $L = 2500 \text{ fb}^{-1}$ and $L = 5000 \text{ fb}^{-1}$, respectively. At first two stages, it will be enable to study the gauge sector, Higgs and top physics with a high precision. At the third stage, the most precise investigation of the SM, as well as new physics will be possible [37, 38].

At the CLIC, it is possible to study not only e^+e^- scattering but also $\gamma\gamma$ collisions with real photons. These photon beams are given by the Compton backscattering of laser photons off linear electron beams. The physics potential of a linear collider is greatly enhanced with polarized beams [39]. The SM backgrounds may be reduced by a factor of five if the electron beam has a polarization of 80%. Searches for new physics can also be enhanced when

using polarization beams. The CLIC accelerator conceptual design includes a source to produce a polarized electron beam and all elements necessary to transport the beam to the IP without loss of polarization. An electron beam polarization of 80% is expected for the baseline CLIC experimental programme.

In our recent paper [36], the axion induced LBL scattering of the *unpolarized* CB photons was investigated. In the present paper, we propose to study the same process with ingoing *polarized* CB photon beams. A summation over outgoing photons is assumed. The main goal is to demonstrate that the CLIC bounds on the ALP parameters can be improved if one considers the polarized LBL scattering.

2 Polarized real photon beams

As was already mentioned above, $\gamma\gamma$ -interactions with real photons can be examined at the CLIC. Real photons beams are obtained by the Compton backscattering of laser photons off linear electron beams. Most of these real scattered photons have high energy, and the $\gamma\gamma$ luminosity turns out to be of the same order as the one for e^+e^- collision [40]. That is why one gets a large cross section for the LBL scattering of the real photons.

The spectrum of backscattered photons is given by helicities of initial laser photon and electron beam as follows

$$f_{\gamma/e}(y) = \frac{1}{g(\zeta)} \left[1 - y + \frac{1}{1-y} - \frac{4y}{\zeta(1-y)} + \frac{4y^2}{\zeta^2(1-y)^2} + \lambda_0 \lambda_e r \zeta (1-2r)(2-y) \right], \quad (1)$$

where

$$g(\zeta) = g_1(\zeta) + \lambda_0 \lambda_e g_2(\zeta), \quad (2)$$

$$g_1(\zeta) = \left(1 - \frac{4}{\zeta} - \frac{8}{\zeta^2} \right) \ln(\zeta + 1) + \frac{1}{2} + \frac{8}{\zeta} - \frac{1}{2(\zeta + 1)^2}, \quad (3)$$

$$g_2(\zeta) = \left(1 + \frac{2}{\zeta} \right) \ln(\zeta + 1) - \frac{5}{2} + \frac{1}{\zeta + 1} - \frac{1}{2(\zeta + 1)^2}, \quad (4)$$

and

$$\zeta = \frac{4E_e E_0}{M_e^2}, \quad y = \frac{E_\gamma}{E_e}, \quad r = \frac{y}{\zeta(1-y)}. \quad (5)$$

Here E_γ is the scattered photon energy, E_0 and λ_0 are the energy, and the helicity of the initial laser photon beam, E_e , and λ_e are the energy and helicity of the initial electron beam before CB. Note that the variable y reaches its maximum value 0.83 when $\zeta = 4.8$. The helicity of the CB photons,

$$\xi(E_\gamma, \lambda_0) = \frac{\lambda_0(1-2r)(1-y+1/(1-y)) + \lambda_e r \zeta [1 + (1-y)(1-2r)^2]}{1-y+1/(1-y) - 4r(1-r) - \lambda_e \lambda_0 r \zeta (2r-1)(2-y)}, \quad (6)$$

has the highest value when $y \simeq 0.83$. In what follows, we will consider two cases:

$$\begin{aligned} (\lambda_0^{(1)}, \lambda_e^{(1)}; \lambda_0^{(2)}, \lambda_e^{(2)}) &= (1, -0.8; 1, -0.8), \\ (\lambda_0^{(1)}, \lambda_e^{(1)}; \lambda_0^{(2)}, \lambda_e^{(2)}) &= (1, +0.8; 1, +0.8), \end{aligned} \quad (7)$$

where the superscripts 1 and 2 enumerate the beams. As for the integrated luminosities for the baseline CLIC energy stages, we will take them from Ref. [41], see Tab. 1.

		Unpolarized	$\lambda_e = -0.8$	$\lambda_e = +0.8$
Stage	\sqrt{s} , GeV	\mathcal{L} , fb $^{-1}$	\mathcal{L} , fb $^{-1}$	\mathcal{L} , fb $^{-1}$
1	380	1000	500	500
2	1500	2500	2000	500
3	3000	5000	4000	1000

Table 1. The CLIC energy stages and integrated luminosities for the unpolarized and polarized electron beams.

As one can see from Tab. 1, for the polarized electron beams the luminosities are noticeably smaller than those for the unpolarized beams, especially for the first two energy stages and $\lambda_e = 0.8$.

Numerical estimates have shown that for $\sqrt{s} = 380$ GeV the total cross sections almost coincide with the SM cross sections [36]. That is why, we will do our calculations for the collision energies $\sqrt{s} = 1500$ GeV (2nd stage of the CLIC) and $\sqrt{s} = 3000$ GeV (3rd stage of the CLIC).

3 Light-by-light production of ALP

We will consider a Lagrangian with the CP-even coupling of the pseudoscalar ALP (in what follows, denoted as a) to photons, and the ALP coupling to

fermions,

$$\mathcal{L}_a = \frac{1}{2} \partial_\mu a \partial^\mu a - \frac{1}{2} m_a^2 a^2 + \frac{a}{f} F_{\mu\nu} \tilde{F}^{\mu\nu} + \frac{\partial_\mu a}{2f} \sum_\psi c_\psi \bar{\psi} \gamma^\mu \psi, \quad (8)$$

where $F_{\mu\nu}$ is the electromagnetic tensor, $\tilde{F}_{\mu\nu} = (1/2)\varepsilon_{\mu\nu\rho\sigma} F^{\rho\sigma}$ its dual, c_ψ is a dimensionless constant. Note that, contrary to the QCD axion, the ALP does not couple to the gluon anomaly. The ALP-photon coupling f defines the ALP decay width into two photons

$$\Gamma(a \rightarrow \gamma\gamma) = \frac{m_a^3}{4\pi f^2}, \quad (9)$$

and the decay rate of the ALP to fermions,

$$\Gamma(a \rightarrow \bar{\psi}\psi) = \frac{m_a m_\psi^2}{8\pi} \left(\frac{c_\psi}{f}\right)^2 \sqrt{1 - \frac{4m_\psi^2}{m_a^2}}, \quad (10)$$

where m_ψ is the fermion mass. As one can see from eqs. (9), (10), for $m_a \gg m_\psi$, and $c_\psi = \mathcal{O}(1)$ the full width of the ALP will be mainly defined by its decay into two photons. In general, the ALP branching $\text{Br}(a \rightarrow \gamma\gamma)$ can be less than 1.

The differential cross section of the diphoton production with the initial polarized CB photons is defined by [42]

$$\begin{aligned} \frac{d\sigma}{d\cos\theta} &= \frac{1}{128\pi s} \int_{x_{1\min}}^{0.83} \frac{dx_1}{x_1} f_{\gamma/e}(x_1) \int_{x_{2\min}}^{0.83} \frac{dx_2}{x_2} f_{\gamma/e}(x_2) \\ &\times \left\{ \left[1 + \xi \left(E_\gamma^{(1)}, \lambda_0^{(1)} \right) \xi \left(E_\gamma^{(2)}, \lambda_0^{(2)} \right) \right] |M_{++}|^2 \right. \\ &\quad \left. + \left[1 - \xi \left(E_\gamma^{(1)}, \lambda_0^{(1)} \right) \xi \left(E_\gamma^{(2)}, \lambda_0^{(2)} \right) \right] |M_{+-}|^2 \right\}, \quad (11) \end{aligned}$$

where $x_i = E_\gamma^{(i)}/E_e$ ($i = 1, 2$) are the energy fractions of the CB photon beams, $x_{1\min} = p_\perp^2/E_e^2$, $x_{2\min} = p_\perp^2/(x_1 E_e^2)$, p_\perp is the transverse momentum of the final photons. Here \sqrt{s} is the center of mass energy of the e^+e^- collider, while $\sqrt{s x_1 x_2}$ is the center of mass energy of the backscattered photons. The amplitudes $|M_{++}|$ and $|M_{+-}|$ are obtained by summations over the helicities of the outgoing photons in the helicity amplitudes,

$$\begin{aligned} |M_{++}|^2 &= |M_{++++}|^2 + |M_{++--}|^2, \\ |M_{+-}|^2 &= |M_{+--+}|^2 + |M_{-++-}|^2. \end{aligned} \quad (12)$$

We have used P-, T-, and Bose symmetries. In its turn, each of the amplitudes is a sum of the ALP and SM terms,

$$M = M_a + M_{\text{SM}} . \quad (13)$$

As the main SM background, we will take into account both W -loop and fermion-loop contributions

$$M_{\text{SM}} = M_f + M_W . \quad (14)$$

The explicit analytical expressions for SM helicity amplitudes in the right-hand side of eq. (12), both for the fermion and W -boson terms, are too long. That is why we do not present them here. They can be found in [36] (see also [23]). In order to reduce the SM background, we will impose the cut on a rapidity of the final state photons, $|\eta_{\gamma\gamma}| < 2.5$. Finally, a possible background with fake photons from decays of π^0 , η , and η' is negligible in the signal region.

In Figs. 2 and 3 the total cross sections for the process $\gamma\gamma \rightarrow \gamma\gamma$ with the unpolarized and polarized CB initial photons are shown as functions of the minimal transverse momenta of the final photons $p_{t,\text{min}}$. In Fig. 2 the invariant energy is taken to be $\sqrt{s} = 1500$ GeV, the ALP mass m_a and its coupling f are chosen to be equal to 1200 GeV and 10 TeV, respectively. In order to reduce the SM background, we have imposed the cut on the invariant energy of the final photons $W = m_{\gamma\gamma} > 200$ GeV. The cross sections are presented for two values of the ALP branching $\text{Br} = \text{Br}(a \rightarrow \gamma\gamma)$. The curves in the left, middle and right panels correspond to the helicity of the initial electron beam before CB $\lambda_e = 0$ (unpolarized case), $\lambda_e = -0.8$, and $\lambda_e = 0.8$, respectively. The SM predictions are also presented. The total cross sections for $\sqrt{s} = 3000$ GeV are shown in Fig. 3. As one can see, the deviation from the SM gets higher as $p_{t,\text{min}}$ increases, especially for $\lambda_e = 0.8$ (-0.8), if $\sqrt{s} = 1500$ (3000) GeV. Let us note that for $\sqrt{s} = 1500$ GeV, $\lambda_e = -0.8$, the total cross section for the polarized beams is even less than the unpolarized total cross section. The same is true for $\sqrt{s} = 3000$ GeV and $\lambda_e = 0.8$.

Figs. 4 and 5 demonstrate the dependence of the total cross sections on the ALP mass both for unpolarized and polarized electron beams for $\sqrt{s} = 1500$ GeV, two values of the coupling constant f , and two values of the ALP branching $\text{Br}(a \rightarrow \gamma\gamma)$. The total cross sections for $\sqrt{s} = 3000$ GeV are shown in Figs. 6 and 7. All the curves have sharp peaks near point $m_a = 1200$ GeV. As mentioned after eq. (5), the maximum value of the ratio

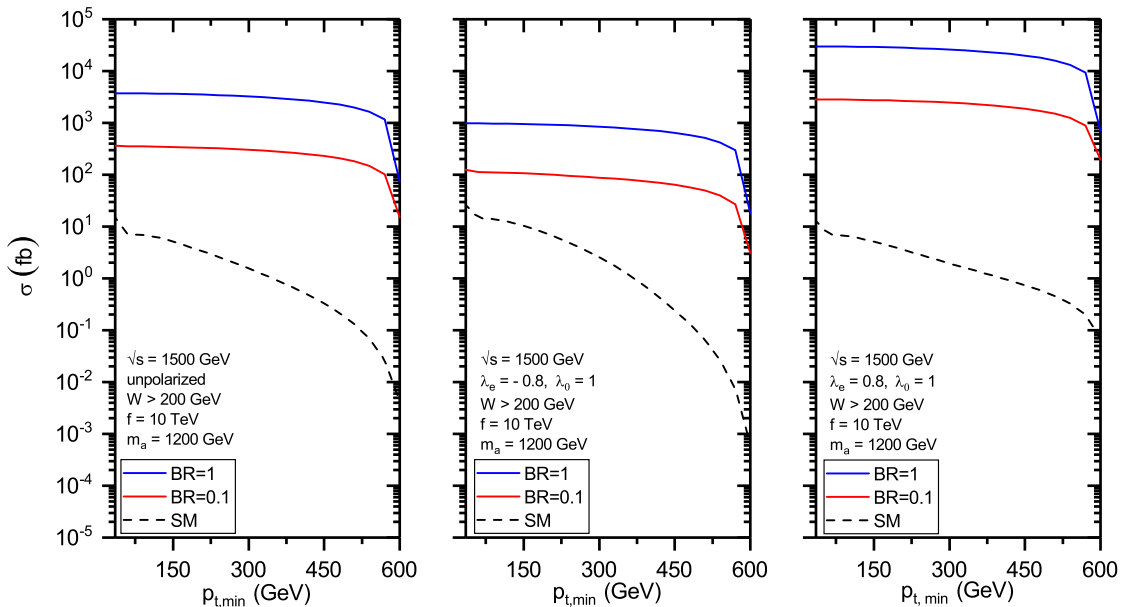


Figure 2: The total cross sections for the process $\gamma\gamma \rightarrow \gamma\gamma$ at the CLIC as functions of the transverse momenta cutoff $p_{t,\min}$ of the final photons for the invariant energy $\sqrt{s} = 1500$ GeV. Left panel: unpolarized case. Middle panel: the helicity of the electron beam is $\lambda_e = -0.8$. Right panel: the helicity of the electron beam is $\lambda_e = 0.8$.

E_γ/E_e is equal to 0.83. That is why, a bump around 0.83×1500 GeV = 1245 GeV should be expected, in agreement with Figs. 4, 5. As one can see, for $\sqrt{s} = 1500$ GeV the polarized cross sections exceed the unpolarized cross sections by an order of magnitude. Unfortunately, due to the relatively small integrated luminosity for the second CLIC stage (see Tab. 1), expected bounds on m_a and f appears to be even less stronger than corresponding bounds for the unpolarized case. Thus, we have to deal with the third energy stage of the CLIC. For $\sqrt{s} = 3000$ GeV the ratio of the polarized cross section to unpolarized one is approximately equal to 2.5.

One can see that the cross sections in Figs. 6, 7 are very sensitive to the parameter m_a in the interval $m_a = 1000 - 2500$ GeV, in which it is approximately two orders of magnitude greater than for m_a outside of this mass region. An approximate formula for the cross section with the CB initial

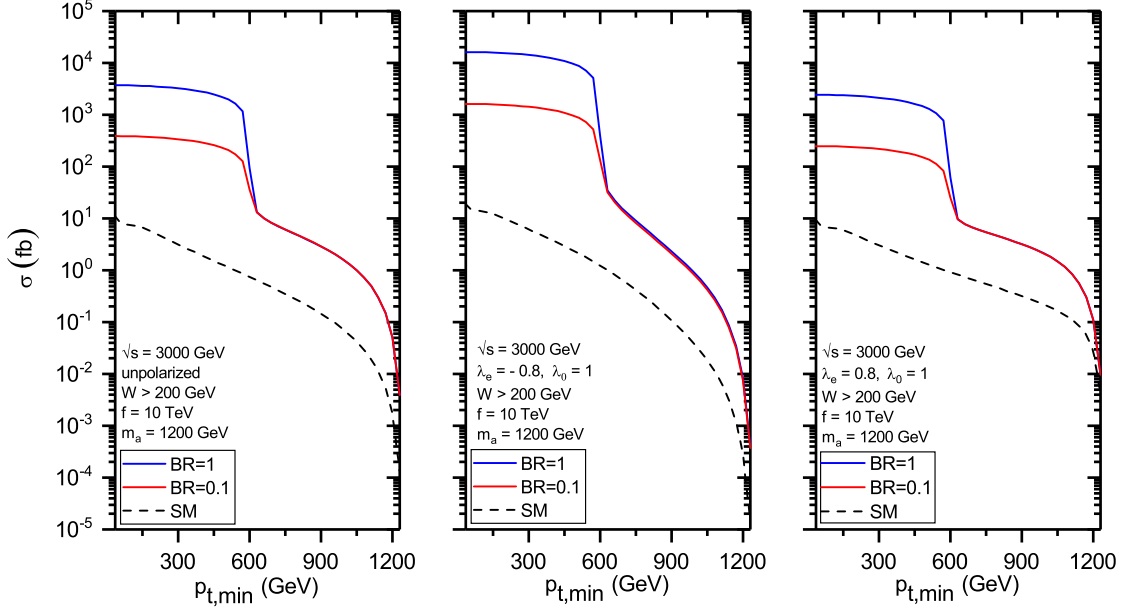


Figure 3: The total cross sections for the process $\gamma\gamma \rightarrow \gamma\gamma$ at the CLIC as functions of the transverse momenta cutoff $p_{t,\min}$ of the final photons for the invariant energy $\sqrt{s} = 3000$ GeV. Left panel: unpolarized case. Middle panel: the helicity of the electron beam is $\lambda_e = -0.8$. Right panel: the helicity of the electron beam is $\lambda_e = 0.8$.

photons can be obtained, which explains a non-trivial dependence of the cross section on the ALP mass m_a , its coupling constant f and $\text{Br}(a \rightarrow \gamma\gamma)$ in the mass region $1000 - 2500$ GeV. The point is that a dominant contribution to the cross section comes from s -channel terms in the matrix element M . To illustrate this point, let us put

$$M = \frac{4}{f^2} \frac{s^2}{s - m_a^2 + im_a\Gamma_a}. \quad (15)$$

The calculations show that the most important energy region is a resonance region $s \sim m_a^2$ in which

$$|M|^2|_{s \sim m_a^2} \sim \frac{m_a^6}{f^4 \Gamma_a^2}. \quad (16)$$

Since our matrix element (15) depends only on s , the cross section of the

subprocess $\gamma\gamma \rightarrow \gamma\gamma$ is given by the integral

$$\sigma = \frac{1}{4E_e^2} \int ds \frac{1}{16\pi s} |M|^2. \quad (17)$$

Let us estimate the contribution to σ from the resonance region

$$m_a^2 - Cm_a\Gamma_a \leq s \leq m_a^2 + Cm_a\Gamma_a, \quad (18)$$

where C is a constant of order $O(1)$. Then we get

$$\sigma = \frac{1}{f^2} \frac{m_a^2}{E_e^2} \text{Br}(a \rightarrow \gamma\gamma) \int_{-C}^C dx \frac{1}{x^2 + 1}. \quad (19)$$

As a result, we find for $C = 1$ that

$$\sigma \simeq 0.6 \left(\frac{\text{TeV}}{f}\right)^2 \left(\frac{m_a}{E_e}\right)^2 \text{Br}(a \rightarrow \gamma\gamma) \text{ fb}. \quad (20)$$

This formula gives a correct dependence of the cross section on the parameters f , m_a and $\text{Br}(a \rightarrow \gamma\gamma)$ in the mass region 1100 – 2500 GeV, see Figs. 6 and 7. Note that σ is proportional to $1/f^2$ (20), while simple dimensional arguments would give us $1/f^4$ dependence. Let us underline that the above considerations are not applicable outside the mass region 1100 – 2500 GeV.

As already mentioned above, the cross sections are very sensitive to the parameter m_a in the interval $m_a = 1000 - 2500$ GeV, in which it is approximately two orders of magnitude greater than for m_a outside of this mass region, see Figs. 6, 7. It is not surprising that this is the region where the value of the ALP coupling constant f is mostly restricted by the polarized LBL process. The exclusion region is presented in the left panel of Fig. 8 in comparison with the unpolarized case is shown in the right panel of this figure. We have used the following formula for calculating the statistical significance (SS) [43]

$$SS = \sqrt{2[(S + B) \ln(1 + S/B) - S]}, \quad (21)$$

where S and B are the numbers of the signal and background events, respectively. It was assumed that the uncertainty of the background is negligible. In order to suppress the SM background, we have applied the cut $p_t > 500$ GeV on the momenta of the final photons.

As it follows from Fig. 8, the best bounds for the LBL scattering at the CLIC are realized for $\text{Br}(a \rightarrow \gamma\gamma) = 1$. Herewith, we have:

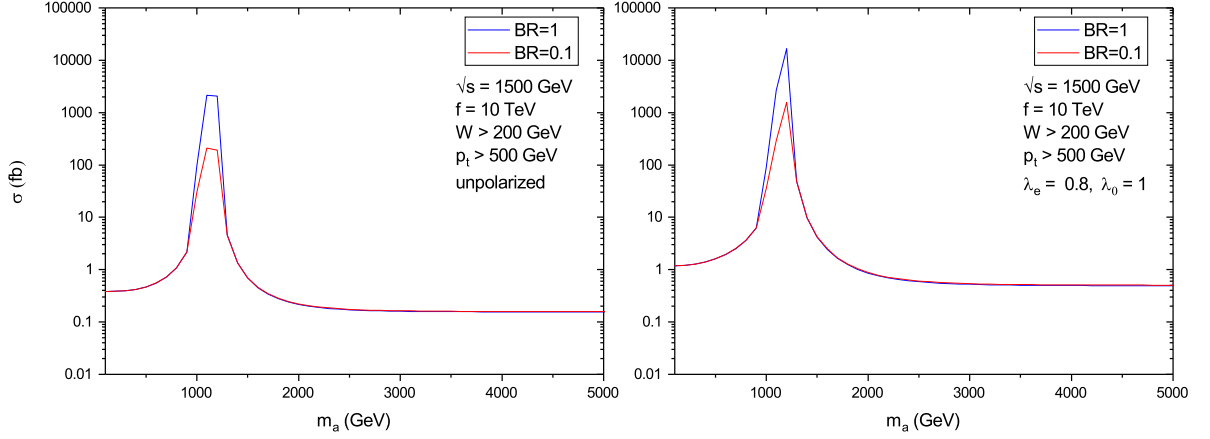


Figure 4: The total cross sections for the process $\gamma\gamma \rightarrow \gamma\gamma$ at the CLIC for the CB initial photons as functions of the ALP mass m_a for $\sqrt{s} = 1500$ GeV and $f = 10$ TeV. Left panel: unpolarized case. Right panel: polarized case, the helicity of the electron beam is equal to $\lambda_e = 0.8$.

- For the mass region $10 \text{ GeV} < m_a < 500 \text{ GeV}$, the polarized and unpolarized upper bounds on f are almost the same, $f^{-1} = 3.0 \times 10^{-2} \text{ TeV}^{-1}$.
- In the interval $500 \text{ GeV} < m_a < 1000 \text{ GeV}$, the polarized bounds are about 1.1 times better than the unpolarized ones. For example, for $m_a = 850 \text{ GeV}$, we find $f^{-1} = 2.65 \times 10^{-2} \text{ TeV}^{-1}$ for the unpolarized case, and $f^{-1} = 2.40 \times 10^{-2} \text{ TeV}^{-1}$ for the polarized case.
- The region $1000 \text{ GeV} < m_a < 2000 \text{ GeV}$ is the best region in which the polarized bounds are on average 1.5 times stronger. For example, for $m_a = 1400 \text{ GeV}$, $f^{-1} = 3.35 \times 10^{-4} \text{ TeV}^{-1}$ for the unpolarized beams, and $f^{-1} = 2.05 \times 10^{-4} \text{ TeV}^{-1}$ for the polarized beams.
- In the mass interval $2000 \text{ GeV} < m_a < 2500 \text{ GeV}$, the unpolarized bounds are 2 times better on average. For instance, for the $m_a = 2400 \text{ GeV}$, we get $f^{-1} = 3.05 \times 10^{-4} \text{ TeV}^{-1}$, and $f^{-1} = 7.35 \times 10^{-4} \text{ TeV}^{-1}$ for the unpolarized and polarized beams, respectively.
- Finally, for $2500 \text{ GeV} < m_a < 5000 \text{ GeV}$ the unpolarized bounds are 1.2 times better on average. In particular, for $m_a = 3500 \text{ GeV}$, we

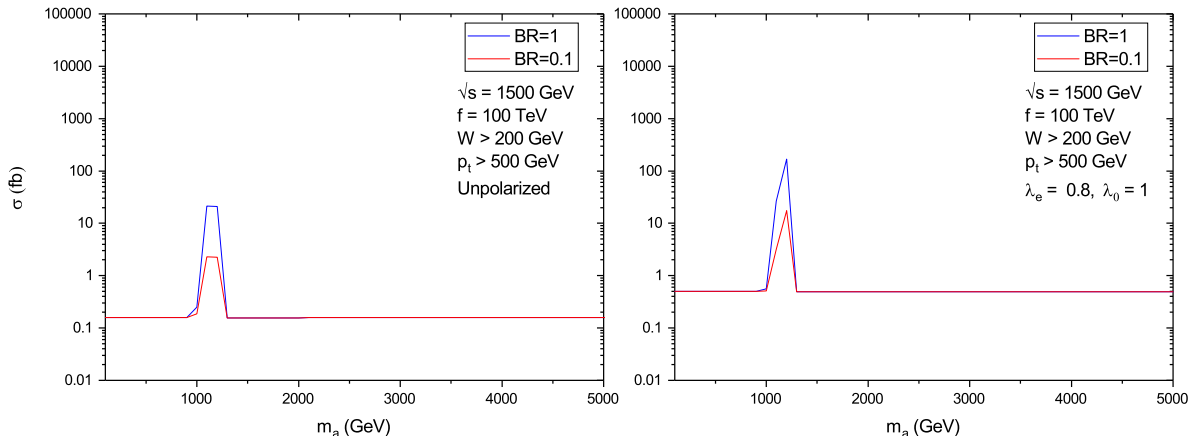


Figure 5: The same as in Fig. 4, but for $f = 100$ TeV.

find $f^{-1} = 3.35 \times 10^{-2} \text{ TeV}^{-1}$ for the unpolarized beams, while $f^{-1} = 4.20 \times 10^{-2} \text{ TeV}^{-1}$ for the polarized beams.

4 Conclusions

In the present paper, the light-by-light scattering with the ingoing *polarized* Compton backscattered photons at the CLIC, induced by the axion-like particles has been studied. The total cross sections are calculated for the e^+e^- collider energies 1500 GeV and 3000 GeV. The cross sections are presented as functions of the ALP mass m_a , its coupling constant f , and ALP branching into two photons $\text{Br}(a \rightarrow \gamma\gamma)$. By combining the results obtained with the results on the *unpolarized* light-by-light scattering derived recently in Ref. [36], we have to make the following conclusions:

1. First energy stage of the CLIC ($\sqrt{s} = 380$ GeV):
The SM contribution completely dominates the axion induced contribution for $f = 10$ TeV in the mass interval $m_a = 10 - 5000$ GeV. Any search of the ALPs is thus meaningless in this mass region.
2. Second energy stage of the CLIC ($\sqrt{s} = 1500$ GeV):
The axion contribution dominates the SM one both for the unpolarized and polarized ingoing CB photons. For the electron beam helicity

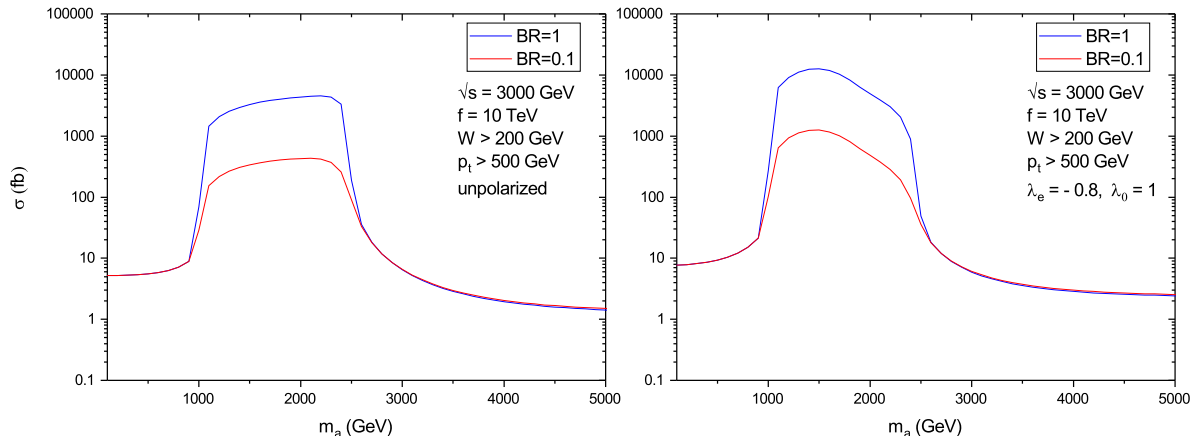


Figure 6: The total cross sections for the process $\gamma\gamma \rightarrow \gamma\gamma$ at the CLIC for the CB initial photons as functions of the ALP mass m_a for $\sqrt{s} = 3000$ GeV and $f = 10$ TeV. Left panel: unpolarized case. Right panel: polarized case, the helicity of the electron beam is equal to $\lambda_e = -0.8$.

$\lambda_e = -0.8$, the cross section is even smaller than the unpolarized cross section, compare the middle and left panels of Fig. 2. But for $\lambda_e = 0.8$ the polarized cross section exceeds the unpolarized one by order of magnitude, see the right panel of Fig. 2. Nevertheless, due to the relatively small value of the expected integrated luminosity in such a case (500 fb^{-1} , as compared with 2500 fb^{-1} for the unpolarized electron beams), the bounds on m_a and f are less stronger than analogous bounds for the unpolarized LBL collision. Thus, one has no advantages to use the polarized electron beams in searching for heavy ALPs at this energy.

3. Third energy stage of the CLIC ($\sqrt{s} = 3000$ GeV):

For the electron beam helicity $\lambda_e = 0.8$ (right panel of Fig. 3), the cross section is smaller than the unpolarized cross section (left panel of Fig. 3). However, for $\lambda_e = -0.8$ the polarized cross section exceeds the unpolarized cross section by a factor of 2.5, as one can see by comparing the middle and left panels of this figure. Fig. 8 demonstrates us that the bounds on m_a and f are better than recently obtained limits for the unpolarized LBL collision in the mass region $m_a = 500 \text{ GeV} - 2000 \text{ GeV}$. Especially, it takes place in the interval $m_a = 1000 \text{ GeV} - 2000$

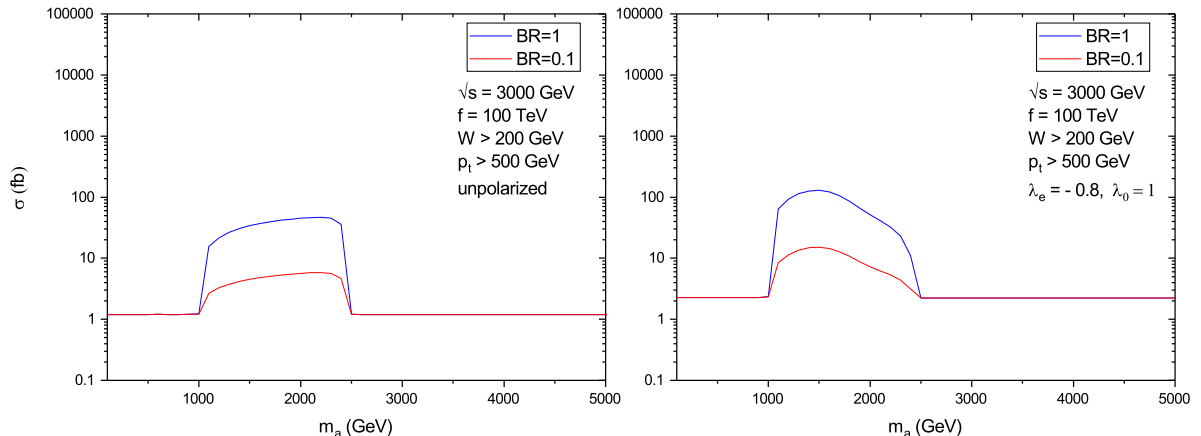


Figure 7: The same as in Fig. 6, but for $f = 100$ TeV.

GeV in which the bounds on f for the polarized beams are on average 1.5 times stronger than the bounds obtained for unpolarized beams.

Our main results are presented in Fig. 9 along with the current exclusion regions. As we can see, for the wide region of the ALP mass, $m_a = 10$ GeV – 5000 GeV, our CLIC bounds are much stronger than the bounds for the ALP production in the LBL scattering at the LHC. They are also stronger than all other exclusion regions for $m_a > 80$ GeV, except for a very small area in between $m_a = 600$ GeV and $m_a = 900$ GeV, see Fig. 9. By comparing our results on the polarized LBL scattering with the unpolarized case, we can conclude that the third energy stage of the CLIC with the polarized electron beams have the greater physical potential to search for heavy ALPs, especially in the ALP mass region 1000 GeV – 2000 GeV.

References

- [1] R.D. Peccei and H.R. Quinn, *CP Conservation in the Presence of Pseudoparticles*, Phys. Rev. Lett. **38**, 1440 (1977).
- [2] R.D. Peccei and H.R. Quinn, Phys. Rev. D, *Constraints imposed by CP conservation in the presence of pseudoparticles* **16**, 1791 (1977).
- [3] S. Weinberg, *A New Light Boson?*, Phys. Rev. Lett. **40**, 223 (1978).

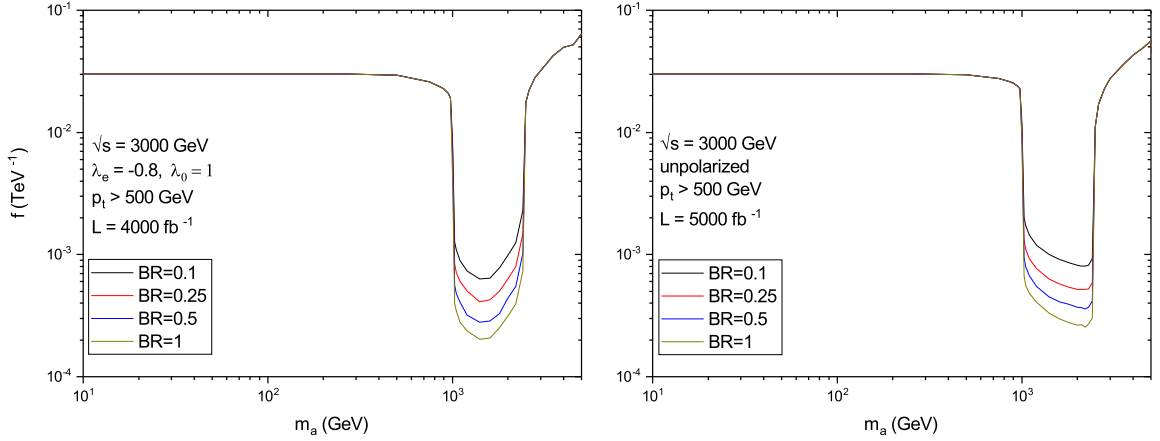


Figure 8: The 95% C.L. CLIC exclusion region for the process $\gamma\gamma \rightarrow \gamma\gamma$ with the CB ingoing photons and invariant energy $\sqrt{s} = 3000$ GeV. Left panel: polarized electron beams with the helicity $\lambda_e = -0.8$; integrated luminosity $L = 4000 \text{ fb}^{-1}$. Right panel: unpolarized electron beams; integrated luminosity $L = 5000 \text{ fb}^{-1}$ [36].

- [4] F. Wilczek, *Problem of Strong P and T Invariance in the Presence of Instantons*, Phys. Rev. Lett. **40**, 279 (1978).
- [5] J. Preskill, M.B. Wise, and F. Wilczek, *Cosmology of the Invisible Axion*, Phys. Lett. B **120**, 127 (1983).
- [6] L.F. Abbott, and P. Sikivie, *A cosmological bound on the invisible axion*, Phys. Lett. B **120**, 113 (1983).
- [7] M. Dine and W. Fischler, *The Not So Harmless Axion*, Phys. Lett. B **120**, 137 (1983).
- [8] K. van Bibber *et al.*, *Design for a practical laboratory detector for solar axions*, Phys. Rev. D **39**, 2089 (1989); S. Moriyama, *Proposal to Search for a monochromatic component of Solar Axion Using ^{57}Fe* , Phys. Rev. Lett. **75**, 3222 (1995).
- [9] E. Aprile *et al.* (XENON Collaboration), *Observation of Excess Electronic Recoil Events in XENON1T*, arXiv:2006.09721.

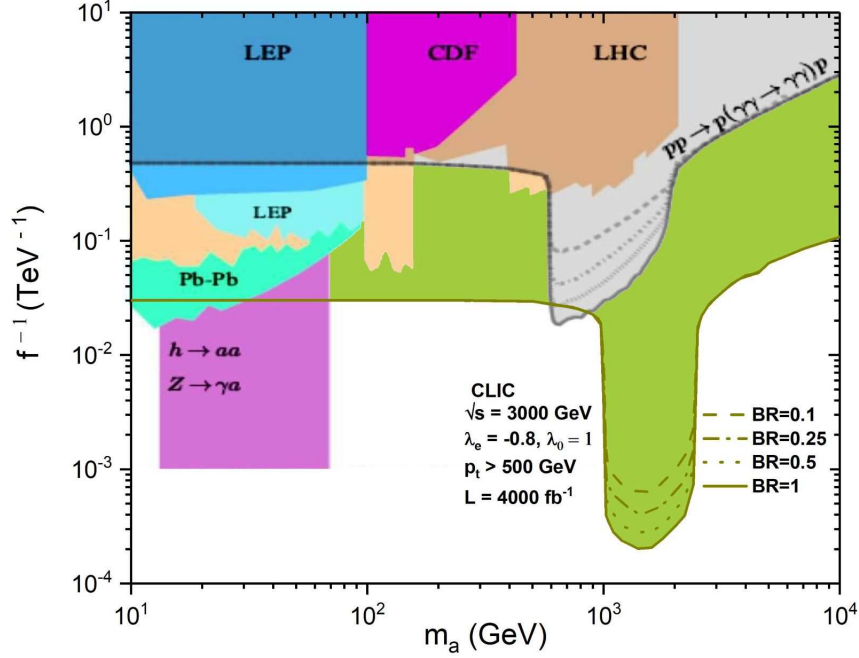


Figure 9: Our prediction for the 95% C.L. exclusion region for the energy $\sqrt{s} = 3000$ GeV, electron beam polarization $\lambda_e = -0.8$, and different values of the ALP branching $\text{Br}(a \rightarrow \gamma\gamma)$ (green area), in comparison with other current exclusion regions.

- [10] P. Svrcek and E. Witten, *Axions In String Theory*, JHEP **06**, 051 (2006).
- [11] J.P. Conlon, *The QCD Axion and Moduli Stabilisation*, JHEP **05**, 78 (2006).
- [12] M.R. Douglas and S. Kachru, *Flux compactification*, Rev. Mod. Phys. **79**, 733 (2007).
- [13] A. Arvanitaki, S. Dimopoulos, S. Dubovsky, N. Kaloper and J. March-Russell, *String Axiverse*, Phys. Rev. D **81**, 123530 (2010).
- [14] B.S. Acharya, K. Bobkov and P. Kumar, *An M-theory Solution to the Strong CP Problem and Constraints on the Axiverse*, JHEP **11**, 105 (2010).

- [15] M. Cicoli, M.D. Goodshell and A. Ringwald, *The type IIB string axiverse and its low-energy phenomenology*, JHEP **10**, 146 (2012).
- [16] J. Halverson, C. Long, B. Nelson and G. Salinas, *On String Theory Expectations for Photon Couplings to Axion-Like Particles*, Phys. Rev. D **100**, 106010 (2019).
- [17] E. Massó and R. Toldrà, *On a light spinless particle coupled to photons*, Phys. Rev. D **52**, 1755 (1997).
- [18] B. Bellazzini *et al.*, *R-axion at colliders*, Phys. Rev. Lett. **119**, 141804 (2017).
- [19] V.A. Rubakov, *Grand unification and heavy axion*, Pis'ma Zh. Exsp. Teor. Fiz. **65**, 590 (1997) [JETP. Lett. **65**, 621 (1997)].
- [20] I.G. Irastorza and J. Redondo, *New experimental approaches in the search for axion-like particles*, Prog. Part. Nucl. Phys. **102**, 89 (2018).
- [21] M. Bauer, M. Neubert and A. Thamm, *Collider Probes of Axion-Like Particles*, JHEP **12**, 044 (2017).
- [22] S. Knapen, T. Lin, H.K. Lou and T. Melia, *Searching for axion-like particles with ultra-peripheral heavy-ion collisions*, Phys. Rev. Lett. **118**, 171801 (2017); *LHC limits on axion-like particles from heavy-ion collisions*, in Proceeding of the PHOTON 2017 Conference, Geneva, Switzerland, 22-26 May, 2017, eds. D. d'Enterria, A. de Roeck and M. Mangano, vol. 1, 2018, pp. 65-68 (arXiv:1709.07110).
- [23] C. Baldenegro, S. Fichet, G. von Gersdorff and C. Royon, *Searching for axion-like particles with proton tagging at the LHC*, JHEP **06**, 131 (2018); *Probing the anomalous $\gamma\gamma Z$ coupling at the LHC with proton tagging*, JHEP **06**, 142 (2017).
- [24] C. Baldenegro, S. Hassani, C. Royon and L. Schoeffel, *Extending the constraint for axion-like particles as resonances at the LHC and laser beam experiments*, Phys. Lett. B **795**, 339 (2019).
- [25] M. Bauer, M. Heiles, M. Neubert and A. Thamm, *Axion-like particles at future colliders*, Eur. Phys. J. C **79**, 74 (2019).

- [26] M. Aaboud *et al.* (ATLAS Collaboration), *Evidence for light-by-light scattering in heavy-ion collisions with the ATLAS detector at the LHC*, Nat. Phys. **13**, 852 (2017).
- [27] G. Aad *et al.* (ATLAS Collaboration), *Observation of Light-by-Light Scattering in Ultrapерipheral Pb+Pb Collisions with the ATLAS Detector*, Phys. Rev. Lett. **123**, 052001 (2019).
- [28] D. d’Enterria *et al.* (CMS Collaboration), *Evidence for light-by-light scattering in ultraperipheral PbPb collisions at $\sqrt{s} = 5.02$ TeV*, Nucl. Phys. A **982**, 791 (2019).
- [29] R.O. Coelho *et al.*, *Exclusive and diffraction $\gamma\gamma$ production in PbPb collisions at the LHC, HE-LHC and FCC*, Eur. Phys. J. C **80**, 488 (2020).
- [30] R.O. Coelho *et al.*, *Production of axionlike particles in PbPb collisions at the LHC, HE-LHC and FCC: A phenomenological analysis*, Phys. Lett. **806**, 135512 (2020).
- [31] S. Atağ, S.C. İnan and İ. Şahin, *Extra dimensions in photon-induced two lepton final states at the CERN LHC*, Phys. Rev. D **80**, 075009 (2009).
- [32] S. Atağ, S.C. İnan and İ. Şahin, *Extra dimensions in $\gamma\gamma \rightarrow \gamma\gamma$ process at the CERN-LHC*, JHEP **09**, 042 (2010).
- [33] S.C. İnan and A.V. Kisselev, *Probe of the Randall-Sundrum-like model with the small curvature via light-by-light scattering at the LHC*, Phys. Rev. D **100**, 095004 (2019).
- [34] H. Braun *et al.* (CLIC Study Team), *CLIC 2008 parameters*, CERN-OPEN-2008-021, CLIC-NOTE-764.
- [35] M.J. Boland *et al.* (CLIC and CLICdp Collaborations), *Updated baseline for a staged Compact Linear Collider*, CERN-2016-004, arXiv:1608.07537.
- [36] S.C. İnan and A.V. Kisselev, *A search for axion-like particles in light-by-light scattering at the CLIC*, arXiv:2003.01978.

- [37] D. Dannheim *et al.*, *CLIC e^+e^- Linear Collider Studies*, arXiv:1208.1402.
- [38] *The CLIC Potential for New Physics*, eds. J. de Blas *et al.*, CERN Yellow report: Monographs, Vol. 3/2018, CERN-2018-009-M (CERN, Geneva, 2018); R. Franceschini, *Beyond the Standard Model physics at CLIC*, arXiv:1902.10125.
- [39] G. A. Moortgat-Pick *et al.*, *The role of polarised positrons and electrons in revealing fundamental interactions at the Linear Collider*, Phys. Rep. **460**, 131 (2008).
- [40] I.F. Ginzburg, G.L. Kotkin, V.G. Serbo and V.I. Telnov, *Colliding γe and $\gamma\gamma$ beams based on the single-pass e^+e^- colliders (of VLEPP Type)*, Nucl. Instrum. Meth. **205**, 47 (1983); I.F. Ginzburg, G.L. Kotkin, S.L. Panfil, V.G. Serbo and V.I. Telnov, *Colliding γe and $\gamma\gamma$ beams based on single-pass e^+e^- accelerators II. Polarization effects, monochromatization improvement, *ibid.* **219**, 5 (1984).*
- [41] R. Franceschini, P. Roloff, U. Schnoor and A. Wulzer, *The Compact Linear e^+e^- Collider (CLIC): Physics Potential*, arXiv:1812.07986.
- [42] O. Çakir, K.O. Ozansoy, *Unparticle searches through gamma-gamma scattering*, Eur. Phys. J. C **56**, 279-285 (2008).
- [43] G. Cowan, K. Cranmer, E. Gross and O. Vitells, *Asymptotic formulae for likelihood-based tests of new physics*, Eur. Phys. J. C **71**, 1554 (2011).